Optical control of electron spin coherence in CdTe/(Cd,Mg)Te quantum wells

E. A. Zhukov,[1,2] D. R. Yakovlev,[1,3] M. M. Glazov,[3] L. Fokina,[1] G. Karczewski,[4] T. Wojtowicz,[4] J. Kossut,[4] and M. Bayer[1]
[1]*Experimentelle Physik 2, Technische Universität Dortmund, 44221 Dortmund, Germany*
[2]*Faculty of Physics, M. V. Lomonosov Moscow State University, 119992 Moscow, Russia*
[3]*Ioffe Physical-Technical Institute, Russian Academy of Sciences, 194021 St. Petersburg, Russia*
[4]*Institute of Physics, Polish Academy of Sciences, PL-02668 Warsaw, Poland*
(Received 13 December 2009; revised manuscript received 23 May 2010; published 16 June 2010)

Optical control of the spin coherence of quantum well electrons by short laser pulses with circular or linear polarization is studied experimentally and theoretically. For that purpose the coherent electron spin dynamics in a *n*-doped CdTe/(Cd,Mg)Te quantum well structure was measured by time-resolved pump-probe Kerr rotation, using resonant excitation of the negatively charged exciton (trion) state. The amplitude and phase shifts of the electron spin beat signal in an external magnetic field, that are induced by laser control pulses, depend on the pump-control delay and polarization of the control relative to the pump pulse. Additive and nonadditive contributions to pump-induced signal due to the control are isolated experimentally. These contributions can be well described in the framework of a two-level model for the optical excitation of the resident electron to the trion.

DOI: 10.1103/PhysRevB.81.235320 PACS number(s): 78.55.Cr, 73.21.Fg, 72.25.Dc

I. INTRODUCTION

Semiconductor spintronics relies on the possibility to control electron spins by non-magnetic methods so that high-frequency manipulation on time scales approaching the pico- and femtosecond ranges, well below the coherence time, becomes feasible.[1–3] To this end optical methods have been considered to be most promising. Substantial experimental and theoretical efforts have been directed toward studies addressing optical orientation of electron spins as well as generation and control of electron spin coherence in semiconductor nanostructures.

Pump-probe techniques are very convenient tools to study coherent spin dynamics.[4] Thereby a circularly polarized pump pulse, typically with duration between 100 fs and 1 ps, generates the electron spin orientation, which is subsequently monitored by the weaker linearly polarized probe pulse delayed relative to the pump pulse. The rotation of the probe polarization plane measured, e.g., in transmission (Faraday rotation) or reflection (Kerr rotation) geometry is directly proportional to the electron spin polarization along the optical axis. In a perpendicular external magnetic field, the coherent spin precession of the electrons can be monitored giving access to the electron spin dephasing times.

Possibilities of optical rotation of the electron spin to reach all points on the Bloch sphere by the spin vector have been widely discussed. But only very recently this goal has been achieved for a single quantum dot,[5,6] an ensemble of singly charged (In,Ga)As quantum dots[7] and a CdTe/(Cd,Mg)Te quantum well (QW).[8] In these experiments care was taken that only the spin coherence initiated by the pump is manipulated, but no additional spin coherence is created by the control. This was achieved when the control energy was either detuned from the pump energy, so that the pulses have no spectral overlap, or by means of 2π control pulses. It was demonstrated that the polarization vector undergoes a full revolution on the Bloch sphere.

In this paper, we report on a different regime, where the control and pump photon energies coincide. It was shown that in this regime the spin coherence of Mn spins in CdTe/(Cd,Mn)Te QWs as a result of the optical excitation shows additive contributions of the pump and control pulses.[9] It can be enhanced or suppressed by proper choice of the control polarization and time delay relative to the pump pulse. Here we investigate the electron spin coherence in CdTe/(Cd,Mg)Te QWs containing a low density electron gas, for which spin coherence is generated by resonant excitation of the negatively charged exciton (trion) resonance.[10,11] We found that the control effect is determined by additive and nonadditive mechanisms, whose relative strengths depend on the electron spin polarization initiated by the pump. Surprisingly, a linearly polarized control pulse causes a very efficient suppression of the electron spin coherence, while excitation with such a pulse does not lead to any spin polarization. The developed quantitative theory allows us to explain these experimental data quantitatively.

The paper is organized as follows. After introducing the experiment in Sec. II, in Sec. III experimental results for the optical control with circularly and linearly polarized control pulses are described. Also a qualitative model of the effect of a linearly polarized control on the signal suppression is presented. Section IV is devoted to quantitative theoretical considerations based on a two-level system for the electron-trion optical excitation. The experimental results are compared with the modeling in Sec. V. Here, we also discuss possible reasons for deviations between the experiment and theory at high powers of control.

II. EXPERIMENTAL TECHNIQUES

The studied CdTe/$Cd_{0.78}Mg_{0.22}$Te QW heterostructure (sample 031901D) was grown by molecular-beam epitaxy on top of a 2 μm CdTe buffer layer deposited on a (100)-oriented GaAs substrate. It contains 5 periods, each of them consisting of a 110-nm-thick $Cd_{0.78}Mg_{0.22}$Te barrier and a 20-nm-thick CdTe QW. An additional 110-nm-thick barrier was grown on top of this layer sequence to reduce the

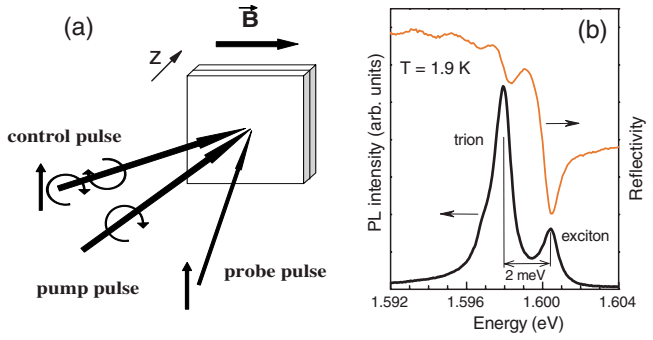

FIG. 1. (Color online) (a) Scheme of the three-pulse time-resolved Kerr rotation experiment. (b) Photoluminescence and reflectivity spectra of a 20-nm-thick $CdTe/Cd_{0.78}Mg_{0.22}Te$ QW. PL was measured under nonresonant *cw* excitation with photon energy of 2.33 eV.

influence of surface charges on the confined electronic states in the QWs. The barriers include 15 nm layers doped by Iodine donors, which are separated by 20 nm spacers from the QWs. These modulation doped layers provide electrons being collected in the QWs, where two-dimensional electros gases (2DEGs) with a low density of about $n_e=2\times10^{10}$ cm^{-2} form. This sample has a slightly larger electron density compared to its partner sample 031901C ($n_e=1.1\times10^{10}$ cm^{-2}) grown on the same substrate by a wedge growth technique[12] which has been studied in Ref. 10. The optical properties of both samples are, however, similar to each other, see Refs. 10, 13, and 14 for details.

The measurements were performed in magnetic fields up to 7 T applied perpendicular to the structure growth axis, $\mathbf{B}\perp\mathbf{z}$ (Voigt geometry). The sample was immersed in pumped liquid Helium at a temperature of $T=1.9$ K.

Time-resolved pump-probe Kerr rotation (KR) technique was used to study the coherent spin dynamics of the resident QW electrons.[10] Two mode-locked Ti:Sapphire lasers synchronized with each other generated the 1.5 ps pump and control pulses (spectral width of about 1 meV) at a repetition frequency of 75.6 MHz. The probe beam was split off from the pump laser, as sketched in Fig. 1(a). For the experiments reported here both lasers were tuned to the same photon energy corresponding to the trion resonance.

The electron spin coherence was excited by the pump and control pulses, for which different polarization configurations were used: The control was either co- or cross-circularly polarized with respect to the pump of fixed circular σ^+ polarization, or it was linearly polarized. The induced spin coherences were monitored by the reflected linearly polarized probe pulse, for which the angle of Kerr rotation was measured by a balanced photodetector interfaced by a lock-in amplifier, after sending it through a polarization sensitive Glan-Thompson beam splitter. The time delay between pump and probe pulses could be varied up to 7 ns by a mechanical delay line. A second delay line was used to set a fixed delay of the control pulse relative to the pump pulse. This delay could be changed up to $t_{pc}\leq2$ ns in order to tune the phases of the spin coherences initiated pump and control with respect to each other.

Two protocols of pump and control beam modulation were used. First we present experiments, where the signals are mainly given by the additive effect of the pump and control actions. Here both pump beam and control beam were modulated by a chopper at a frequency of 1 kHz, so that the detected Kerr rotation signal reflects the effect of both beams. These measurements are described in Secs. III A–III C.

In order to study the "nonadditive" effect of the control on the pump induced signal we used a protocol in which only pump beam was modulated. It was sent through a photoelastic modulator operated at 50 kHz frequency so that the polarization was modulated between σ^+ and σ^-. The polarization of the control beam was constant in time. The Kerr rotation signal was detected at the pump modulation frequency of 50 kHz, which allows us to suppress the additive contribution to the electron spin polarization induced by the non-modulated control beam. These results are reported in Sec. III E.

III. EXPERIMENTAL RESULTS AND DISCUSSION

Photoluminescence (PL) and reflectivity spectra of the studied QW structure are shown in Fig. 1(b). The heavy-hole exciton (X) and negatively charged trion (T) resonances are clearly seen as minima in the reflectivity spectrum and as lines in the PL spectrum. They are separated by 2 meV, which corresponds to the trion binding energy.[11,15] The broadening of these lines is mainly due to exciton and trion localization on QW width fluctuations. From the relative oscillator strengths of the exciton and trion resonances in the reflectivity spectrum we evaluate the resident electron concentration in the QW as $n_e=2\times10^{10}$ cm^{-2} using the method described in Ref. 16.

A typical Kerr rotation signal measured at a magnetic field of 0.5 T is shown in Fig. 2 by curve (a). The σ^+ circularly polarized pump pulse hits the sample at zero time delay and induces coherent spin precession of the resident electrons about the external magnetic field. The precession is reflected by the periodically oscillating Kerr signal amplitude $K(t)$. The oscillation period corresponds to the electron Larmor frequency $\omega_e=\mu_B g_e B/\hbar$ with an electron g factor $|g_e|=1.64$, which is in good agreement with literature data.[17] Here μ_B is the Bohr magneton. The g-factor value was obtained from fitting the experimental data by an exponentially decaying harmonic function[4]

$$K(t)=A\exp\left(-\frac{t}{T_2^*}\right)\cos(\omega_e t). \quad (1)$$

Here A corresponds to the signal amplitude, T_2^* is the dephasing time describing the signal decay. The evaluated dephasing time $T_2^*=4.2$ ns is considerably longer than the trion recombination times in the range of 30–100 ps in CdTe-based QWs,[10] which allows us to ascribe the Kerr signal to resident electrons.

A. Effect of circularly polarized control on signal amplitude

We turn now to the main topic of the present paper, namely the effect of control pulses, delayed by a time t_{pc} relative to the pump pulse, on the electron spin coherence

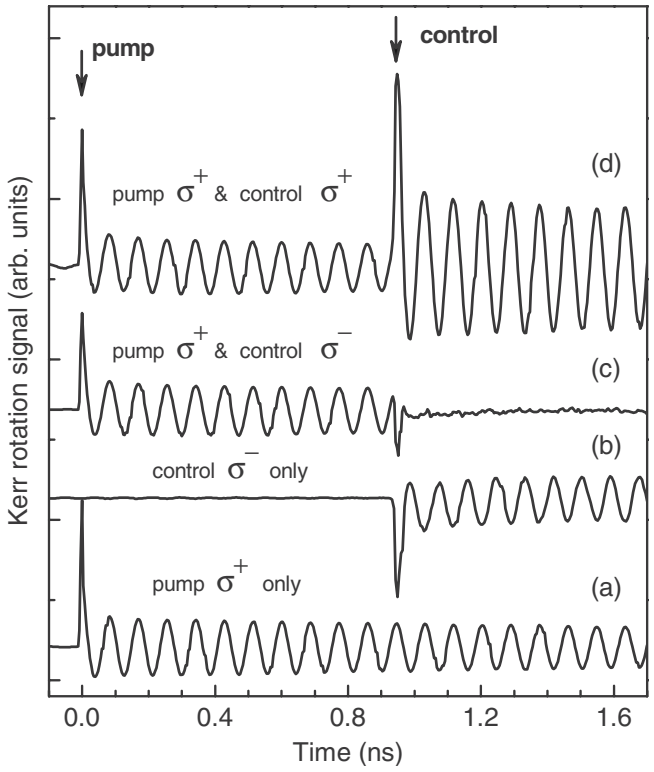

FIG. 2. Kerr rotation signals measured by degenerate pump-control-probe spectroscopy resonant with the trion energy: (a) Only pump pulse with σ^+ polarization and density of 0.3 W/cm^2. Evaluated T_2^*=4.2 ns. (b) Only control pulse with σ^- polarization and density of 0.3 W/cm^2. (c) σ^+ pump pulse and σ^- control pulse joint excitation. (d) σ^+ pump pulse and σ^+ control pulse joint excitation. B=0.5 T, T=1.9 K. For (b)–(d) t_{pc}=0.96 ns and φ=0.

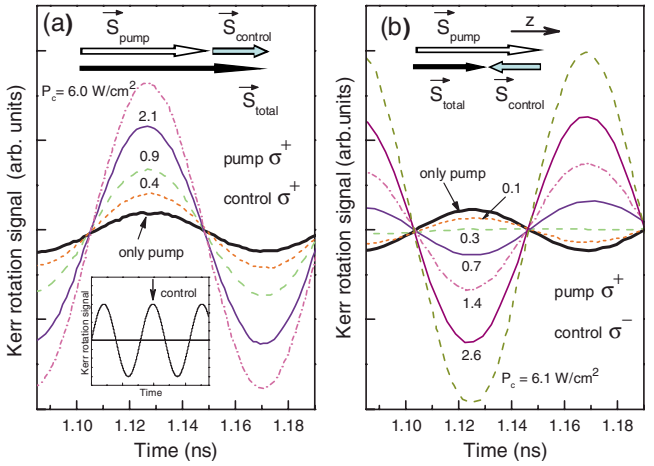

FIG. 3. (Color online) Kerr rotation signals measured for various control pulse power (P_c) at B=0.5 T. Pump is σ^+ polarized with power of P_p=0.3 W/cm^2: (a) σ^+ control pulse; (b) σ^- control pulse. Arrow in the inset marks time moment of control pulse arrival at t_{pc}=0.87 ns, which corresponds to φ=0. Arrows in the panels show schematically the contributions to electron spin polarization induced by the pump ($\mathbf{S}_{\text{pump}}$), the control ($\mathbf{S}_{\text{control}}$) and the result of their joint action ($\mathbf{S}_{\text{total}}$).

generated by the pump. The modifications induced by the control depend critically on the reduced phase φ with which the control hits the pump excited electron spin coherence. This reduced phase is defined as $\omega_e t_{pc}=\varphi+2\pi N$, where N is an integer corresponding to the number of full spin precession periods during the pump-control delay, and $0\leq\varphi<2\pi$.

We describe first the pump-probe experiments, in which a circularly polarized control was used. We also focus on the signal amplitude modifications induced by the control, the changes of the phase are discussed in Sec. III B. To that end we adjust the delay t_{pc} such that phase φ=0 is achieved, when the Kerr signal amplitude $K(t)$ is maximum. At a magnetic field of 0.5 T this condition is fulfilled, e.g., at t_{pc}=0.87 ns or t_{pc}=0.96 ns. The latter example one can see in Fig. 2 by comparing curves (a) and (b). For co-polarized pump and control pulses (both σ^+) of the same power the Kerr signal is enhanced about twice after control action, see curve (d). This is the expected result, as in this case the electron spin polarization generated by the control has the same orientation as the one generated by the pump after a few full revolutions about the field. In contrast, cross polarization of the pump (σ^+) and control (σ^-) pulses leads to full suppression of the electron spin precession signal, as shown by curve (c). In this case the electron polarizations generated by the pump and control are antiparallel and compensate each other.

Note that for the low excitation density regime presented in Fig. 2 only a small fraction of the resident electrons is affected by the pump and control pulses. In this case the joint action of the pump and control can be described such that each of them generates spin coherence for two independent subensembles of electrons. The experimentally measured Kerr rotation signal results from their independent contributions, which make either additive or subtractive effect on the observed signal. Note, that a very similar behavior has been previously reported for the Mn spin coherence in CdTe/(Cd,Mn)Te QWs.[9]

Detailed results for the effect of control power on the Kerr signal amplitude for co- and cross-polarizations of pump and control are given in Fig. 3. The phase for control pulse arrival was chosen to be φ=0, as in Fig. 2. Therefore, the spin polarizations induced by the pump ($\mathbf{S}_{\text{pump}}$) and the control ($\mathbf{S}_{\text{control}}$) are either parallel or antiparallel to each other for co- and cross-polarizations, respectively. The resultant polarization ($\mathbf{S}_{\text{total}}$) along the z axis is reduced or increased, as shown schematically in the corresponding panels of Fig. 3.

The Kerr amplitude increases for the co-polarized configuration shown in Fig. 3(a), in line with the intuitive expectations. It decreases for the cross-polarized case given in Fig. 3(b), crosses the zero level when the control power becomes about equal to the pump power and then shows increasing negative values. These dependencies can be seen in detail in Fig. 4, where the dependence of the Kerr amplitude on control power is plotted. To determine the spin beat amplitudes the signals after the control pulse arrival were fitted by Eq. (1). Triangles and circles give the experimental data for co- and cross-polarized pump and control pulses, respectively. The absolute changes of the KR amplitudes relative to the dashed line are larger for the cross-polarized configuration. This results from the faster saturation of the electron spin for co-polarized excitation compared to the cross-

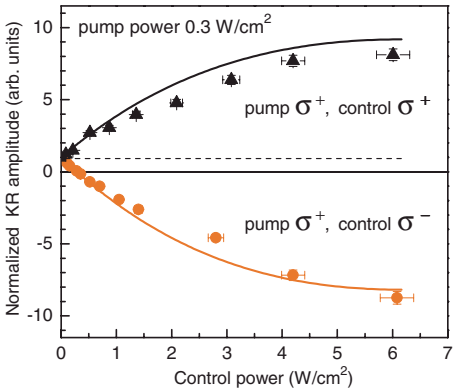

FIG. 4. (Color online) Amplitude of Kerr rotation signal as function of control power. The amplitude is taken after the time moment of control pulse arrival for co- and cross-polarization of pump and control: triangles—pump σ^+ and control σ^+ (regime of amplification); circles—pump σ^+ and control σ^- (regime of suppression). B=0.5 T, t_{pc}=0.87 ns, and φ=0. Solid lines show calculated amplitudes of the signals according to Eq. (16), with details presented in Sec. IV and discussed in Sec. V A. Dashed line shows the pump induced KR amplitude without control.

polarized case. We will discuss that in more details in Sec. V A.

B. Effect of circularly polarized control on signal phase

When the control pulse acts on the pump induced polarization at an arbitrary phase φ, not only the amplitude of the Kerr rotation signal changes, but also the phase will be shifted by an angle θ after the control pulse arrival. Corresponding experimental data are shown in Fig. 5(a), where we chose cross-polarization for pump and control and $\varphi=\pi/2$. The inset in Fig. 5(b) shows schematically that for these experimental conditions the signal after the control pulse is expected to show a negative phase shift, i.e., to shift to earlier delays. The signal after control pulse arrival can be described by Eq. (1) when replacing $\cos(\omega_e t)$ by $\cos(\omega_e t+\theta)$:

$$K(t) = A\,\exp\left(-\frac{t}{T_2^*}\right)\cos(\omega_e t+\theta). \tag{2}$$

In agreement with our qualitative expectations, the signal phase shown in Fig. 5(b) by the filled circles decreases and saturates at $\theta=-\pi/2$ for control powers strongly exceeding the pump power. The open circles in Fig. 5(b) show the signal phase evaluated from the experimental signal amplitudes without and with control using the simple additive model depicted in the inset of Fig. 5(a). As one can see from scheme the phase shift θ is determined in this case of perpendicular orientation of $\mathbf{S}_{\text{pump}}$ and $\mathbf{S}_{\text{control}}$ by

$$\theta = \arctan(S_{\text{control}}/S_{\text{pump}}). \tag{3}$$

The overall tendency of the dependences shown by the closed and open circles is the same. However, they deviate considerably from each other for control powers exceeding 0.5 W/cm^2. This evidences some nonadditive contribution of the control to the spin coherence generated by the pump, which we will discuss in detail below.

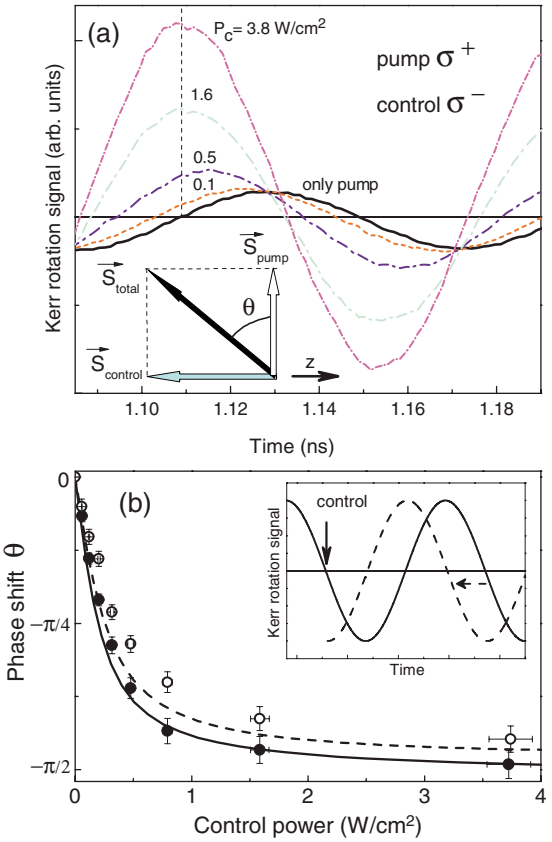

FIG. 5. (Color online) (a) Kerr rotation signals measured for different control powers (P_c): pump (σ^+, 0.15 W/cm^2), control (σ^-). Inset shows scheme of the excited electron spin polarizations. B=0.5 T, t_{pc}=0.89 ns, and $\varphi=\pi/2$. (b) Phase shift of Kerr rotation signal as function of control power. Closed circles show phase shift determined from fitting the experimental data using Eq. (2). Open circles show values calculated from the experimental data using the spin composition model Eq. (3). Lines show the phase of spin beats calculated from the microscopic model, Eq. (22) (solid line) and from the additive model (dashed lines) Eq. (23), for details refer to Sec. IV B. Inset shows schematically the modification of the pump-induced signal (solid line) by the control pulse arriving such that $\varphi=\pi/2$, inducing a phase shift of the resultant signal (dashed line).

The results in Fig. 6 have been collected to confirm the conclusion drawn from the data in Fig. 5, that the phase shift of the Kerr rotation signal is mainly controlled by the ratio of the pump and control generated spin polarizations, $S_{\text{control}}/S_{\text{pump}}$. An increase of the control power for constant pump power causes a shift of the signal to earlier times, compare curves 1 and 2. This corresponds to an increase of the phase shift value, as shown by the left diagram. In turn, a pump power increase for constant control power (curves 2 and 3 and the right diagram) induces a signal shift to later times. For the chosen power densities these transformations are dominated by the additive mechanism.

C. Effect of linearly polarized control

In our experimental geometry it is not expected that linearly polarized light would induce any spin polarization of

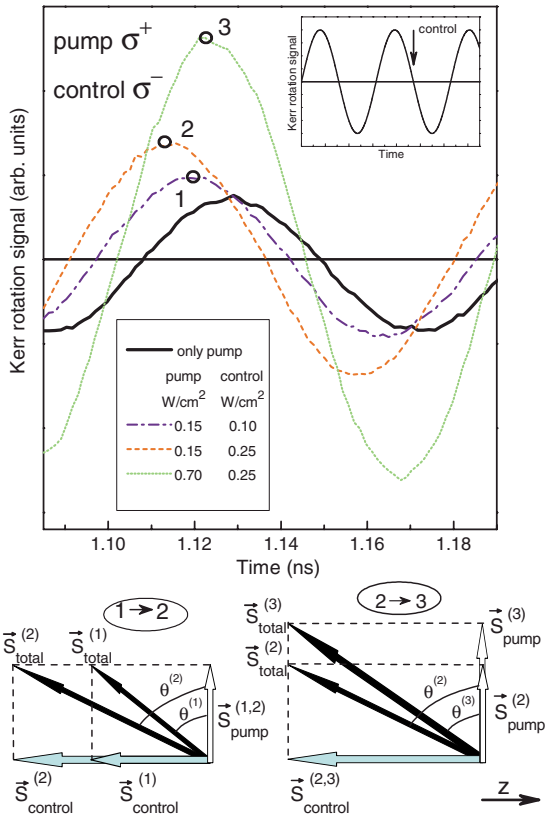

FIG. 6. (Color online) Kerr rotation signals measured at different pump (σ^+) and control (σ^-) powers. B=0.5 T, t_{pc}=0.89 ns, and $\varphi=\pi/2$. Inset illustrates the control pulse arrival time (arrow) relative to the KR signal generated by the pump. Two bottom diagrams illustrate the changes of the phase shift θ of the KR signal.

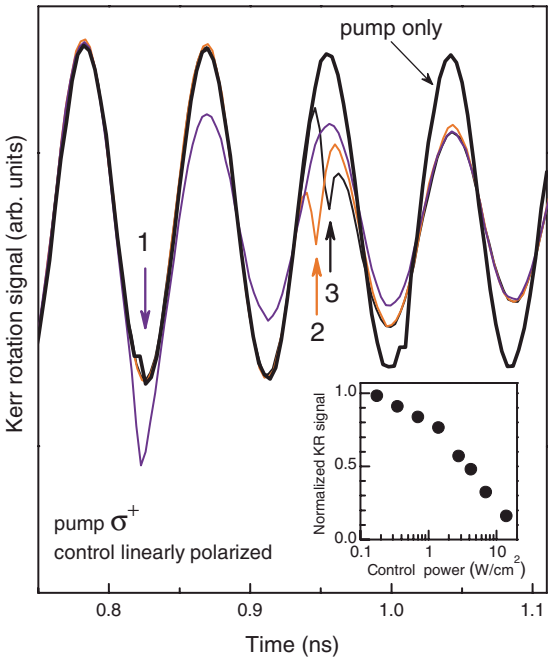

FIG. 7. (Color online) Kerr rotation signals measured at different time moments of control pulse arrival (indicated by arrows) for σ^+ polarized pump with P_p=2.2 W/cm^2 and linearly polarized control with P_c=2.2 W/cm^2. B=0.5 T. Arrival times of the control pulses are shown by arrows: (1) t_{pc}=0.82 ns, $\varphi=\pi$; (2) t_{pc}=0.95 ns, $\varphi=1.8\pi$; and (3) t_{pc}=0.96 ns, φ=0. Inset illustrates suppression of KR signal amplitude with increasing control power. The amplitude is normalized to its value without control.

the resident electrons. Indeed, we did not find any signal for a linearly polarized pump. However, we observed that the electron spin polarization induced by a circularly polarized pump is strongly sensitive to a linearly polarized control. One can see in Fig. 7 that irrespective of the delay t_{pc} the Kerr rotation signal is suppressed by a linearly polarized control. The suppression effect increases for higher control powers as shown in the inset. One should note that this effect changes only the signal amplitude but does not induce any phase shift θ, independently of t_{pc}. The suppression is clearly a nonadditive effect: generation of spin coherence by the control pulse is absent, but the signal is still modified. These experimental findings can be explained by the qualitative model presented in the following section.

D. Qualitative model consideration of linearly polarized control action

In order to develop a qualitative picture of the spin depolarization by the *linearly* polarized control we consider the simple model of a spin ensemble described in Ref. 10. It is assumed that the control pulse is tuned in the vicinity of the trion resonance. We represent the linearly polarized pulse as a superposition of two circularly polarized ones and assume that at the hit time of the control pulse there are n_+ electrons with spin z component 1/2 and n_- electrons with spin z component $-1/2$. We assume that the control pulse arrives at the maximum (φ=0) or the minimum ($\varphi=\pi$) of the pump-induced spin beats, i.e., there are no in-plane spin components at the moment of control pulse arrival.

The absorption of the σ^+ component of the linearly polarized light generates n_+W singlet trions by exciting the same number of s_z=+1/2 resident electrons. Here W is the probability of singlet trion formation per electron due to control pulse action. Analogously, the σ^- component of the linearly polarized light generates n_-W singlet trions by exciting the same number of s_z=−1/2 electrons. Provided the hole spin-flip time is much shorter than the trion radiative lifetime the electrons bound to trions are left unpolarized after trion recombination. Therefore, the total spin of the ensemble is decreased by

$$\delta S_z = S_z^{(a)} - S_z^{(b)} = -\frac{n_+ - n_-}{2} W = -S_z^{(b)} W. \tag{4}$$

Here the superscripts (a) and (b) correspond to the spin z component after and before the control pulse arrival, respectively. The z projection of the total spin of the electron ensemble after control pulse arrival is given by

$$S_z^{(a)} = (1 - W) S_z^{(b)}. \tag{5}$$

Clearly, the probability of singlet trion formation is $0 \le W \le 1$ so that the electron spin after the control pulse is smaller

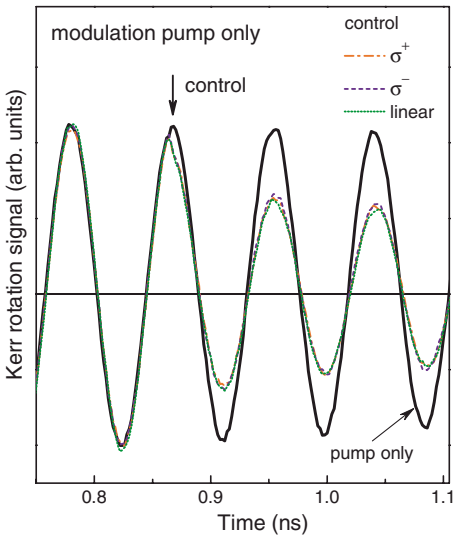

FIG. 8. (Color online) Nonadditive effect on Kerr rotation signals measured for different control polarizations (σ^+, P_c=3.5 W/cm^2) when only the pump beam is modulated (P_p=0.25 W/cm^2). Arrow indicates the time moment of control pulse arrival at t_{pc}=0.87 ns, φ=0. B=0.5 T.

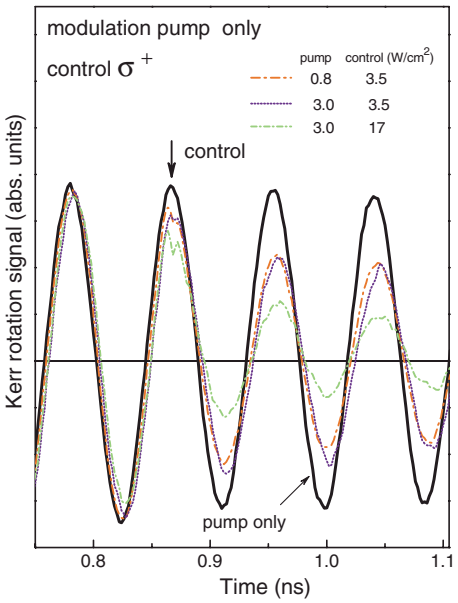

FIG. 9. (Color online) Nonadditive effect on Kerr rotation signals measured at various pump and control (σ^+) powers (pump beam modulation only). Signals are normalized by the pump power to simplify comparison with each other. Thick solid line is pump only signal for P_p=0.25 W/cm^2. B=0.5 T, t_{pc}=0.87 ns, and φ=0.

than the spin before the pulse. It follows therefore that the linearly polarized pump acts as a depolarizer.

E. Nonadditive contribution of control

In this section we address experimentally the question whether a circularly polarized control, similar to a linearly polarized one, can serve as a depolarizer of the induced spin coherence. This will also allow us to obtain in-depth insight into the nonadditive contribution noted in Sec. III B. Our goal here is to study modifications of the pump-induced spin coherence by the control. For that one should exclude Kerr rotation signal that is directly caused by generation of electron spin polarization by the circularly polarized control. It is possible to suppress this signal by implementing the second measurement protocol described in Sec. II. Only the pump beam is modulated in this case and lock-in detection allows us to exclude the direct contribution of the unmodulated control to the detected spin polarization.

One can see in Fig. 8 that also a circularly polarized control decreases the Kerr rotation amplitude, similar to the case of a linearly polarized control. The magnitude of this effect is identical for σ^+ and σ^- polarization of the control and is also independent of the control delay t_{pc} (not shown). It is interesting that the suppression efficiency of the circularly polarized control is equal to the one for a linearly polarized control of the same intensity. This suggests that the responsible mechanism is the same, which is confirmed by the quantitative analysis given below.

In Fig. 9 the effect of the nonadditive contribution is presented for various pump and control powers. The Kerr rotation signals are normalized to their maximum amplitudes before control pulse arrival. Two conclusions follow from these experimental data. First, the suppression efficiency increases with increase of the control power. Second, the suppression efficiency is determined by the control power only, compare the signal amplitudes for different pump powers before and after control arrival for the same control power of 3.5 W/cm^2.

It is worthwhile to note here, that for considerable control powers one may expect the influence of the photogenerated carriers on the dephasing of the electron spin coherence, i.e., on its acceleration after the control pulse arrival. This scenario is not very probable for our case, where the trion resonant excitation is used, as only one electron-hole pair can be generated in vicinity of the localized resident electron. However, in order to avoid such contributions we evaluate the effect of the control pulse on the amplitude of the Kerr rotation signal by fitting the Kerr rotation signal after the control pulse arrival and considering changes in the amplitude at the moment of the arrival. In this case the results became independent of the dephasing time.

IV. QUANTITATIVE THEORY

The quantitative theory of spin manipulation by a control pulse is developed following the methods described in Ref. 18. The electric field of the control pulse can be written as

$$\boldsymbol{E}(\boldsymbol{r},t) = E_{\sigma^+}(\boldsymbol{r},t)\boldsymbol{o}_+ + E_{\sigma^-}(\boldsymbol{r},t)\boldsymbol{o}_- + \text{c.c.}, \tag{6}$$

where $\boldsymbol{o}_\pm$ are the circularly polarized unit vectors related to the unit vectors $\boldsymbol{o}_x \| x$ and $\boldsymbol{o}_y \| y$ by $\boldsymbol{o}_\pm = (\boldsymbol{o}_x \pm i\boldsymbol{o}_y)/\sqrt{2}$. Here the components E_{σ^+} and E_{σ^-} are proportional to the product of the exponential function $\exp(-i\omega_C t)$ with ω_C being the control pulse optical frequency and a smooth envelope. We assume that the optical frequency, ω_C, is close to the trion resonance frequency.

The incident electromagnetic field induces optical transitions between the electron state and the trion state, creating a coherent superposition of them. In accordance with the selection rules σ^+ circularly polarized light creates a superposition of the $+1/2$ electron and $+3/2$ trion states, while σ^- polarized light creates a superposition of the $-1/2$ electron and $-3/2$ trion states. In order to describe these superpositions it is convenient to introduce a four component wave function

$$\Psi = (\psi_{1/2}, \psi_{-1/2}, \psi_{3/2}, \psi_{-3/2}), \tag{7}$$

where the $\pm 1/2$ subscripts denote the electron spin projection and $\pm 3/2$ refer to the spin projection of the hole in the trion. The electron spin polarization is expressed in terms of $\psi_{\pm 1/2}$ as follows

$$S_z = (|\psi_{1/2}|^2 - |\psi_{-1/2}|^2)/2,$$

$$S_x = \mathrm{Re}(\psi_{1/2}\psi^*_{-1/2}),$$

$$S_y = -\mathrm{Im}(\psi_{1/2}\psi^*_{-1/2}). \tag{8}$$

Here Re and Im are real and imaginary parts, respectively. All excited states of the system, such as, e.g., triplet trion states are neglected. In this respect the model is directly applicable to the case of a resident carrier strongly localized in a quantum dot or quantum well imperfection. The role of excited states will be discussed below, in Sec. IV C.

Further, we assume that the delay between the pump and control pulses exceeds by far the radiative lifetime of the trion, hence, just before the control pulse arrival there is a resident electron with precessing spin but no trion. The state of the system just before the control pulse arrival corresponds to the nonzero components $|\psi_{+1/2}|^2 + |\psi_{-1/2}|^2 = 1$ and $\psi_{\pm 3/2} = 0$.

Following the method in Ref. 18 and introducing smooth envelopes for the σ^+ and σ^- polarized components of the control pulse by

$$f_\pm(t) = -\frac{e^{i\omega_C t}}{\hbar}\int d(\boldsymbol{r}) E_{\sigma_\pm}(\boldsymbol{r},t) d^3 r,$$

where $d(\boldsymbol{r})$ is the effective transition dipole, see Eq. (12) in Ref. 18, one may reduce the Schroedinger equation for the four-component wave function to two independent differential equations for $\psi_{\pm 1/2}(t)$, which take the following simple form

$$\ddot{\psi}_{\pm 1/2} - \left[i\omega' + \frac{\dot{f}_\pm(t)}{f(t)} \right] \dot{\psi}_{\pm 1/2} + f_\pm^2(t)\psi_{\pm 1/2} = 0. \tag{9}$$

Here $\omega' = \omega_C - \omega_0$ is the detuning between the control pulse optical frequency and the trion resonance frequency, ω_0. This simple form of Eq. (9) follows from (i) disregarding other excited states of the system and (ii) neglecting the control pulse duration compared to the trion lifetime and the electron spin precession period in magnetic field. Below we discuss the cases of linearly and circularly polarized control pulses.

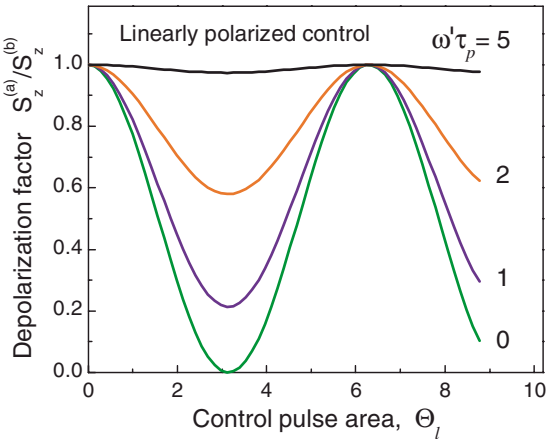

FIG. 10. (Color online) Depolarization factor Q_l^2 as function of control pulse effective area Θ_l calculated for different detunings.

A. Linearly polarized control

In case of a control pulse linearly polarized along the x axis the circular components of the pulse envelope function can be written as

$$f_\pm(t) = \frac{\mu}{\sqrt{2}\cosh\left(\dfrac{\pi t}{\tau_p}\right)}, \tag{10}$$

where the factor $1/\sqrt{2}$ is introduced for convenience, μ characterizes the amplitude of the control pulse and τ_p is its duration. The pulse area is defined as $\Theta = 2\mu\tau_p$. The solution of Eq. (9) can be recast as[18]

$$\psi_{1/2}(+\infty) = \psi_{1/2}(-\infty) Q_l e^{i\Phi_l},$$

$$\psi_{-1/2}(+\infty) = \psi_{-1/2}(-\infty) Q_l e^{i\Phi_l}, \tag{11}$$

where the constants Q_l and Φ_l describe the transformation of the wave function under action of the linearly polarized pulse. For the case of a Rosen and Zener pulse, Eq. (10), one has

$$Q_l^2 = 1 - \frac{\sin^2(\Theta_l/2)}{\cosh^2(\pi y)}, \tag{12}$$

where $\Theta_l = 2\mu\tau_p/\sqrt{2}$ is the effective area of each circularly polarized component of the control pulse, and $y = \omega'\tau_p/(2\pi)$. The expression for the constant Φ_l is rather bulky and is therefore not given here, see Eq. (26) in Ref. 18.

Using the definitions of the spin components, Eqs. (8), one can readily obtain from Eq. (11) that the spin vector of an electron after the control pulse, $\boldsymbol{S}^{(a)}$, is connected with the electron spin vector before the control pulse arrival, $\boldsymbol{S}^{(b)}$, by

$$\boldsymbol{S}^{(a)} = Q_l^2 \boldsymbol{S}^{(b)}, \tag{13}$$

i.e., the spin vector before the control pulse is simply multiplied by some nonnegative quantity $Q_l^2 \leq 1$. If the electron is left behind unpolarized after trion decay, i.e., when the trion lifetime is longer than the hole spin relaxation time, then the total spin of the electron ensemble is decreased, in agreement with the simplified Eq. (5) obtained from qualitative argu-

ments. The dependence of the depolarization factor Q_l^2 on the control pulse area for different detunings between the trion resonance and the control optical frequencies is shown in Fig. 10. The depolarization efficiency shows Rabi oscillations and is larger for small detunings.

In the case of small control power effective pulse area $\Theta_l \ll 1$, and for negligible detuning between the control pulse and the trion resonant frequency, $y \ll 1$, one can represent Q_l^2 in Eq. (12) as

$$Q_l^2 \approx 1 - \frac{(\mu\tau_p)^2}{2}. \tag{14}$$

B. Circularly polarized control

Now we turn to the case of circularly polarized control pulses. For a σ^+ polarized control pulse the envelope function

$$f_+(t) = \frac{\mu}{\cosh\left(\dfrac{\pi t}{\tau_p}\right)}, \quad f_-(t) = 0. \tag{15}$$

The time integrated intensities of the circularly polarized pulse $\propto \int_{-\infty}^{\infty}[f_+^2(t)+f_-^2(t)]\mathrm{d}t$ and of the linearly polarized pulse, Eq. (10), are the same.

Making use of Ref. 18, we obtain the following expressions which link the spin components before and after control pulse arrival,

$$S_z^{(a)} = \mp \frac{1-Q_c^2}{4} + \frac{Q_c^2+1}{2} S_z^{(b)}, \tag{16}$$

$$S_x^{(a)} = Q_c \cos\Phi_c S_x^{(b)} \pm Q_c \sin\Phi_c S_y^{(b)}, \tag{17}$$

$$S_y^{(a)} = Q_c \cos\Phi_c S_y^{(b)} \mp Q_c \sin\Phi_c S_x^{(b)}. \tag{18}$$

Here the upper signs of $\mp$ and $\pm$ correspond to a σ^+ polarized control and the lower signs to a σ^- polarized control. The constant Q_c is given by

$$Q_c^2 = 1 - \frac{\sin^2(\Theta_c/2)}{\cosh^2(\pi y)},$$

where $\Theta_c = \sqrt{2}\Theta_l = 2\mu\tau_p$. For small pulse areas $\Theta_c \ll 1$ and $y \ll 1$

$$Q_c^2 \approx 1 - (\mu\tau_p)^2. \tag{19}$$

The parameter Φ_c describes the phase of the electron wave function acquired due to the control pulse action and describes the spin rotation by an optical pulse. The expression for the constant Φ_c is presented, e.g., in Eq. (26) of Ref. 18.

The modification of the spin z component by a σ^+ control pulse for different pump pulse areas are shown in Fig. 11. Each curve shows the control pulse area dependence for a fixed pump pulse area $\Theta_0 = 2\mu_0\tau_p$, where μ_0 is the amplitude of the pump pulse envelope as defined in Eq. (15). Rabi oscillations with period 2π are clearly seen. Here we assumed that the control pulse arrives at $\varphi = 0$, i.e., in the same

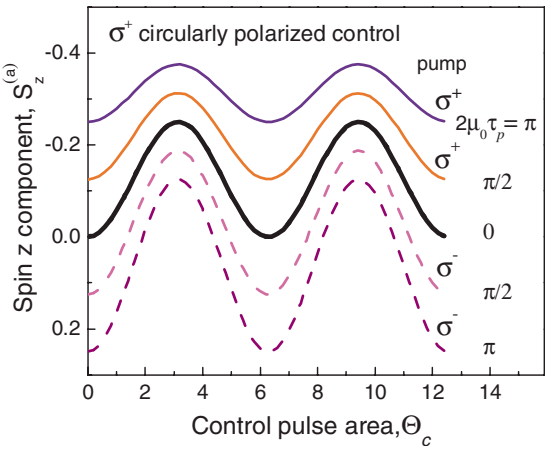

FIG. 11. (Color online) $S_z^{(a)}$ component after σ^+ polarized control pulse arrival as function of control pulse area Θ_c. Different curves correspond to different pump pulse areas $2\mu_0\tau_p$. Solid curves show the case of co-polarized pump and control pulses, dashed curves show the case of cross-polarized pump and control, and the thick solid curve shows the case of control only ($2\mu_0\tau_p = 0$). The control pulse arrives such that $\varphi = 0$.

phase as the pump pulse. Note, that a σ^+ polarized pump results in an electron spin z-projection $S_z < 0$, and corresponds to positive values of the measured Kerr rotation signal, $K(t)$. For convenient comparison of the theoretical and experimental results we invert the direction of the axis of the "spin z component" in the theoretical figures. Here and below the electron spin dephasing is completely neglected in the calculations. The modification of the spin component $S_z^{(a)}$ comprises both additive and nonadditive contributions. Interestingly, for co-polarized pump and control (solid lines) the modification is weaker compared with the cross polarized configuration (dashed lines). This is because the absolute spin value $|S_z|$ is limited by 1/2 and when the spin projection is closer to $-1/2$ (pump and control are co-σ^+ polarized) the effect of the control pulse is weaker.

Time-resolved spin signals calculated for various control pulse powers for the control pulse arrival at different phases of the spin beats are very similar to the experimental data shown in Figs. 3(a), 3(b), and 5(a). For the sake of comparison we plotted in Fig. 12(a) the time dependencies of the spin z component calculated for the control pulse arrival at the zero of spin beats, i.e., phase $\varphi = 3\pi/2$ for the co-circularly polarized pump and control pulses. In accordance with the experiment, Fig. 5(a), both amplitude and phase of the spin beats change with the control power.

Before turning to the detailed comparison of experiment and theory we note that, in agreement with Eq. (16), there are two contributions to the spin z component of an electron after circularly polarized control pulse arrival. The first contribution is an additive one: it changes its sign upon reversal of the circular polarization of the control pulse and it does not depend on the spin state before control pulse arrival. For weak control power, $\mu\tau_p \ll 1$, and negligible detuning, $y \ll 1$, the additive part to $S_z^{(a)}$ is given by, see Eq. (19)

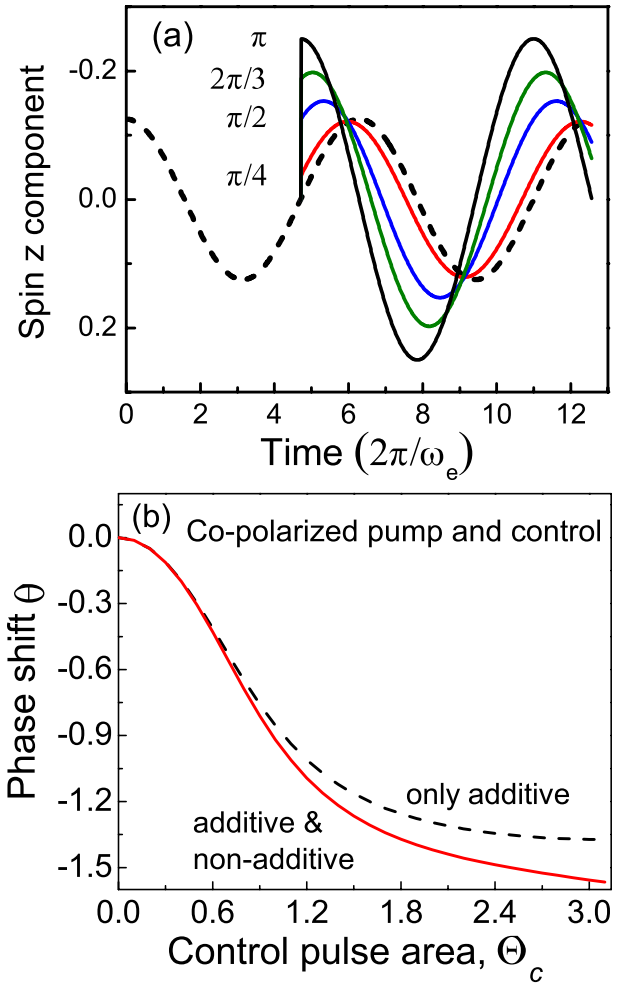

FIG. 12. (Color online) (a) Time resolved dependencies of S_z calculated for the control pulse arrival at beats zero $\varphi=3\pi/2$. Different curves correspond to different amplitudes of the control pulse. The pump and control pulses are co-circularly polarized (σ^+). (b) Phase of the spin beats after control pulse arrival at zero signal ($\varphi=\pi/2$). Pump and control are co-circularly polarized. Solid line gives exact calculation, dashed line is result of an approximate model which accounts for additive contributions by the control only. The absolute spin value for a single electron was taken to be 0.05, which corresponds to a pump area $\Theta_0=2\mu_0\tau_p=0.93$.

$$\mp\frac{1-Q_c^2}{4}\approx\mp\frac{(\mu\tau_p)^2}{4}. \tag{20}$$

This additive contribution equals exactly the spin z component created by a pump pulse of the same power.

Another contribution to the electron spin after control pulse action is a nonadditive one. It can be interpreted as a transformation of the electron spin by the control pulse. This contribution is given by

$$\frac{Q_c^2+1}{2}S_z^{(b)}\approx\left[1-\frac{(\mu\tau_p)^2}{2}\right]S_z^{(b)}, \tag{21}$$

where the last approximate equality holds for weak control power and small detuning. This nonadditive contribution is independent of the circular polarization sign and always decreases the z component of electron spin. The comparison of Eq. (21) with Eqs. (13) and (14) shows that for weak control powers the depolarization of the electron spin z component by circularly and linearly polarized light is the same.

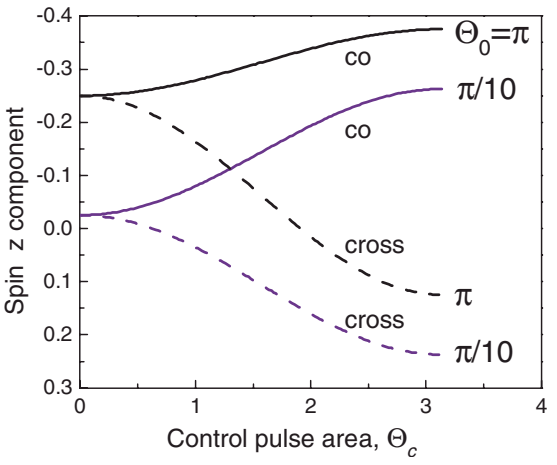

FIG. 13. (Color online) Electron spin z component as function of control pulse area calculated for co-(solid line) and cross-polarized (dashed line) configurations of pump and control for two different pump pulse areas, $\Theta_0=\pi/10$ (blue) and $\Theta_0=\pi$ (black). Phase of control pulse is $\varphi=0$.

The in-plane spin components are also affected by the circularly and linearly polarized control pulses. The absolute value of the in-plane spin projection $S_\perp=\sqrt{S_x^2+S_y^2}$ is decreased by the factor $Q_c\approx 1-(\mu\tau_p)^2/2$ (the latter equality holds for weak control pulses), similar to the case of a linearly polarized control. In addition, the detuned circularly polarized control pulse rotates the in-plane spin by the angle Φ_c around the z axis.

It is noteworthy to analyze the spin beats phase after circularly polarized control arrival at $\varphi=\pi/2$ where the signal amplitude is zero. In order to calculate the spin beats phase we assume that the magnetic field is applied along the x axis. We neglect the detuning between the control pulse optical frequency and the trion resonance frequency. Hence, the phase shift of the spin beats induced by the control is given by

$$\theta=\arctan(S_z^{(a)}/S_y^{(a)}), \tag{22}$$

where the spin precession direction was assumed to be clockwise in the (yz) plane. The dependence of θ on the control pulse area is shown in Fig. 12(b) by the solid line. We compare this phase with the results of the simplified additive model, where we assume that the y spin component is conserved and we take into account the additive contribution of Eq. (16). The phase shift in the additive model is

$$\theta'=\arctan\frac{Q_c^2-1}{4S_y^{(b)}}. \tag{23}$$

This shift is shown by the dashed line in Fig. 12(b). The qualitative behaviors of the two shifts θ and θ' are the same, however, the exact model predicts a stronger phase shift. This results from the suppression of the in-plane components induced by the circularly polarized light.

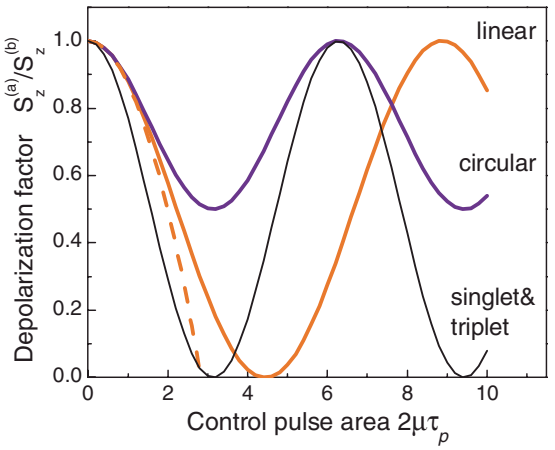

FIG. 14. (Color online) Suppression of the spin z component by circularly (blue solid) and linearly (red solid) polarized control pulses as function of control pulse area. Thin solid line (black) demonstrates spin suppression by a circularly polarized pulse for the case when both singlet and triplet trion transitions are excited with the same probability, Eq. (26) with $\tilde{Q}_c = Q_c$. The detuning between the quantum dot trion resonance and the control optical frequency is zero. Dashed red curve gives the small amplitude asymptotics.

Figure 13 shows the electron spin z component after control pulse arrival, calculated as function of control pulse area for two pump pulse areas and for co- and cross-polarized configurations. We assumed that the control pulse arrives at phase $\varphi=0$ of the spin beats. For a weak pump pulse ($\Theta_0=\pi/10$) the additive contribution by the control is dominant. The modification of the electron spin component is almost the same in the co- and cross-polarized configurations as it mostly scales with control power. The maximum absolute value of the electron spin projection in this case is close to 0.25, in agreement with Eq. (16) for $S_z^{(b)} \ll 1$.

The case of a strong pump pulse, $\Theta_0=\pi$, is different. Figure 13 shows a strong asymmetry for the induced polarizations in the co- and cross-polarized configurations. In the cross-polarized case the change of the spin z component is about the same as for a weaker pump. In the co-polarized configuration the control pulse effect is much weaker. This is because the electron spin coherence generated by the pump pulse is partially suppressed by the control pulse. For this configuration the maximum absolute value of the electron spin z component is $1/4+1/8=0.375$ according to Eq. (16).

Let us also analyze the nonadditive effect by the control pulse for the case when it arrives exactly in the maximum or minimum of the spin beats ($\varphi=0$ or π), i.e., when the in-plane spin components before control pulse arrival are zero $S_x^{(b)}=S_y^{(b)}=0$. In this case the electron spin z component is simply suppressed by the nonadditive contribution, in agreement with Eqs. (16) and (21). The efficiency of the spin depolarization is illustrated in Fig. 14. For small pulse areas indeed the depolarization is the same for the linearly and the circularly polarized control. Rabi oscillations are seen with period 2π for the circularly polarized control and with period $2\sqrt{2}\pi$ for the linearly polarized control. For a circularly polarized control the depolarization is weaker and not complete: one can suppress the spin polarization by no more than a factor of 2, while complete depolarization is possible by linearly polarized light. Note, that complete depolarization is possible for any arrival phase of the control pulse in case of linear polarization.

It is worth to mention that the degree of spin suppression by circularly polarized light is model sensitive. In the following Sec. IV C, we demonstrate that the extension of the model to account for the trion excited states could result in stronger spin suppression by the circularly polarized control.

C. Effects of very strong circularly polarized control pulses

Here we analyze briefly the effect of circularly polarized control pulses of very high intensity. We have seen that the model description in terms of a two-level model gives a complete depolarization of the electron spin by linearly polarized light and partial (by a factor of 2, at most) depolarization by circularly polarized light. This is because the transition for a given circular polarization involves just two levels, the ground electron state and an excited (singlet) trion state. Therefore, only one component of the electron spin is pumped into the trion state and becomes subsequently depolarized, while another one is maintained.

There are other possible excited states in the system, e.g., the triplet trion state, which can be populated by polarized light absorption. In the classical approach[10] this state can be considered as an exciton interacting with a resident electron. Due to the electron spin-flip within a triplet trion a singlet trion state can be formed.

To analyze the nonadditive effect of a circularly polarized control pulse for the case when the triplet trion/exciton can be photocreated, we denote the probability of singlet trion formation via an exciton [as a result of the following process: electron $-1/2$+exciton $(-1/2,3/2)$, afterwards electron spin-flip and formation of $(-1/2,1/2,3/2)$ or $(-1/2,1/2,-3/2)$ trion] by $\tilde{W}$ and the probability of direct singlet trion formation [1/2 electron+photocreated exciton $(-1/2,3/2)$ yields $(-1/2,1/2,3/2)$ trion] as W.

Let us do the analysis for the experimental scenario of Sec. III E where the pump polarization is assumed to be modulated while the control is always σ^+ polarized. If the electron spin before control arrival is 1/2 the electron spin after trion recombination is $(1-W)/2$, because in this case direct singlet trion formation occurs. If the electron spin after control arrival is $-1/2$ then its spin after trion recombination is $-(1-\tilde{W})/2$, since formation of a triplet trion/exciton is required. The detected signal is suppressed compared to the case without control by the factor

$$S_z^{(a)} = \left(1 - \frac{W+\tilde{W}}{2}\right) S_z^{(b)}. \tag{24}$$

At high pump powers both W and $\tilde{W}$ approach unity (see Ref. 10) and the spin after control is completely erased. Clearly, W approaches 1 faster since no electron spin-flip is needed. Therefore one can expect a kind of "two-stage" behavior of suppression: first the spin is suppressed down to

the level $(1-\tilde{W})/2$ of its value before control pulse arrival, and further increase in control power yields complete suppression.

This process can be described quantum mechanically by extending the wave function Ψ, Eq. (7), to allow for the two triplet trion states with total spin projection $\pm 1/2$, formed by two spin down electrons and a 3/2 hole or two spin up electrons and a $-3/2$ hole. For a σ^+ control pulse the electron $-1/2$ is excited into a 1/2 triplet trion, and, following[18] we obtain

$$\psi_{-1/2}(+\infty) = \tilde{Q}_c \exp(i\tilde{\Phi}_c)\psi_{-1/2}(-\infty),$$

$$\psi_{1/2}(+\infty) = Q_c \exp(i\Phi_c)\psi_{1/2}(-\infty).$$

Note that the constants Q_c and $\tilde{Q}_c$ (as well as Φ_c and $\tilde{\Phi}_c$) are different because the triplet trion is usually shifted in energy as compared with the singlet one.[11] If we assume, that after trion recombination the electron is left behind unpolarized, then its spin z component is given by

$$S_z^{(a)} = -\frac{\tilde{Q}_c^2 - Q_c^2}{4} + \frac{\tilde{Q}_c^2 + Q_c^2}{2} S_z^{(b)}. \tag{25}$$

Equation (25) clearly shows that there are both additive and nonadditive contributions to the electron spin z component. The nonadditive contribution is

$$S_z^{(a)} = \frac{\tilde{Q}_c^2 + Q_c^2}{2} S_z^{(b)}. \tag{26}$$

One sees that excitation of the triplet trion state results in additional suppression of the electron spin polarization.

We note that the probability of singlet trion formation by a short pulse is $1-Q_c^2$ and the probability of triplet trion formation is $1-\tilde{Q}_c^2$. Hence, the quantum and classical approaches are equivalent to each other if we take $W=1-Q_c^2$ and $\tilde{W}=1-\tilde{Q}_c^2$.

It is instructive to consider two limiting cases:

(i) Only the triplet trion is excited ($\tilde{Q}_c \neq 0$, $Q_c=0$). The nonadditive spin suppression is fully described by the theory developed in Secs. IV A and IV B by changing $Q_c \to \tilde{Q}_c$, $\Phi_c \to \tilde{\Phi}_c$ and replacing $\mp$ by $\pm$ in Eq. (16). Suppression by the circularly polarized light is possible by a factor 2 only, similar to the situation when only the singlet trion is excited.

(ii) The formation probabilities of the singlet and triplet trions are the same, $Q_c^2=\tilde{Q}_c^2$. The spin suppression factor for circularly polarized control is given by Q_c^2, see Eq. (25), i.e., complete depolarization is possible, see thin solid curve in Fig. 14. It is remarkable that in this case the depolarization effect by linearly and circularly polarized controls of the same area are identical.

V. DISCUSSION

A. Comparison theory and experiment

So far, we have established experimentally and theoretically that the control pulse has, in general, a twofold effect on the electron spin coherence in quantum wells. First, a circularly polarized control pulse generates additional spins and results in an additive contribution to the spin beats. Besides, the control pulse affects the spins that are already polarized by the pump pulse, leading to suppression of the pump-induced spin coherence. The latter effect is possible both for circularly and linearly polarized control pulses.

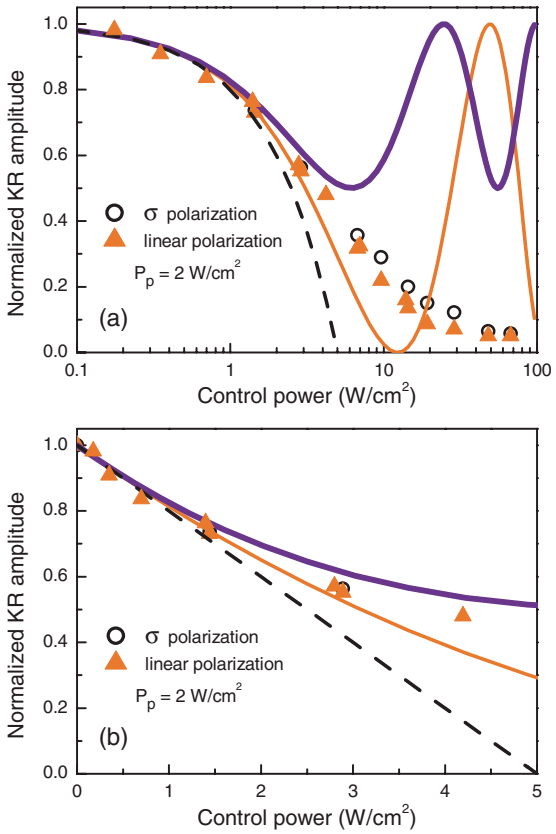

FIG. 15. (Color online) Amplitude of Kerr rotation signal after control pulse arrival normalized to the amplitude before control pulse arrival, $S_z^{(a)}/S_z^{(b)}$. Symbols are experimental data measured for linear polarization of the control pulse (triangles) and for circular polarization (circles). $B=0.5$ T and $T=1.9$ K. Curves are theoretical calculations: suppression for linear polarization (solid red line) and for circular polarization (solid blue line). Dashed curve shows small power asymptotics.

To do a quantitative comparison of the experimental and theoretical results we consider in detail the effect of the spin coherence suppression by linearly and circularly polarized light. Figure 15 shows the suppression efficiency, i.e., the ratio $S_z^{(a)}/S_z^{(b)}$ as function of control pulse power for a linearly polarized control (closed circles) and a circularly polarized control (open circles). We focus on the small control power regime $P_c \leq 5$ W/cm^2 illustrated in detail in Fig. 15(b). In this regime, the efficiency of suppression increases linearly with increasing control pulse power. We fit the experimental data for the linearly polarized control by Eq. (13). We obtain the relation between the control power, P_c, and the linearly polarized control pulse area, Θ_l, see Eq. (12) in the form:

$$P_c = C\Theta_l^2, \tag{27}$$

where the value of the coefficient $C \approx 0.63$ W/cm^2 was determined from the best fit to the experimental data. It was the only fitting parameter in our modeling. The theoretical curve corresponding to the limit of $\Theta_l \ll 1$ is shown by the dashed line in Fig. 15. Further, we use the same value of the parameter C in the whole range of control powers which allows us to avoid introduction of other parameters.

The solid thick red and thin blue lines show the suppression efficiency as function of control power for linear and circular polarizations of the control pulse, respectively. They are calculated for the whole range of experimentally used powers by Eqs. (14) and (21), using the link between the control power and its area from Eq. (27), see Fig. 15(a). The theory reproduces the experimental data well for control powers $P \leq 5$ W/cm^2. For higher powers the discrepancy between experiment and theory is large, the reasons for that are discussed in Sec. V B.

It is worth to note that other experimental data recorded at low-pump powers are in good agreement with the theory. Figure 4 shows the normalized amplitude of the Kerr rotation signal measured as function of control power for co- and cross-polarized configurations. The lines in Fig. 4 show the theoretical calculations obtained from Eq. (16) using the relation between the pulse area and control power Eq. (27) with the same value of $C=0.63$ W/cm^2 as in Fig. 15. Good agreement between the experimental data and theoretical curves is seen. Figure 4 shows that for co-polarization the amplitude of the signal saturates faster than for cross-polarization. This is reasonable, because the spin projection of a single electron is limited by 1/2. Therefore, in co-polarization the spin should saturate faster because spin with projection of the same sign is added and, therefore, the spin reaches the maximum value faster.

We also address the phase shift of the spin beats θ as function of control power, Fig. 5(b). The black circles show the phases of the Kerr signal after control pulse arrival extracted from the experimental data. The dashed curve was calculated in the additive model by Eq. (23), and the solid curve shows the theoretical result taking into account additive and nonadditive effects, Eq. (22). In both calculations the same relation between the pulse area and its power given by Eq. (27) was used. The solid theoretical curve reproduces well the decrease of the phase shift from 0 to $-\pi/2$ and its saturation, confirming that indeed nonadditive effects need to be considered for a comprehensive analysis.

B. Effects of high-control powers

As mentioned above, Fig. 15 shows significant discrepancies between experiment and theory for control powers $P_c \gtrsim 5-10$ W/cm^2. First, Rabi oscillations are not observed experimentally. Second, linearly and circularly polarized control suppress the spin coherence with about same efficiency, while the theory predicts that the suppression for circular polarization should not exceed 50%.

The absence of the Rabi oscillations shows that the quantum model of Ref. 18 used here is not fully applicable for quantum well structures. Indeed, the classical approach developed in Refs. 10 and 19 shows that at high-pumping powers saturation effects become important. The classical approach to the description of spin coherence generation and the quantum approach of Ref. 18, extended here to allow for linearly polarized control pulse, coincide exactly in the limit of weak pump and control powers.[10] With an increase in control power the quantum mechanical approach predicts Rabi oscillations for the control parameters Q_l and Q_c. The quantum approach is justified for quantum dots where electrons and trions preserve their coherence on the time scale of pump or control pulse. The applicability of the quantum approach for quantum wells is governed by the relation between the pulse duration τ_p and the scattering time between different trion states τ_1. If $\tau_p \ll \tau_1$ the two-level model, which describes electron to trion excitation under light pulse action, is valid. Otherwise, if $\tau_p \gtrsim \tau_1$ the trion can scatter to another state during the pulse action and, therefore, the Rabi oscillations become damped.

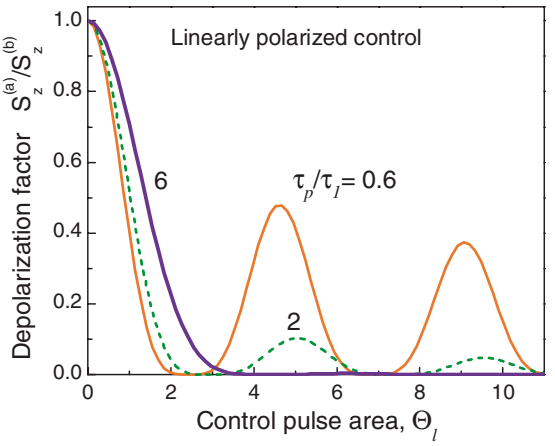

FIG. 16. (Color online) Depolarization factor for a linearly polarized control as function of control pulse area calculated for different ratios of pulse duration τ_p and trion scattering time τ_1: $\tau_p/\tau_1 = 0.6$, 2, and 6.

To illustrate the transition from the quantum to the classical model we performed calculations of the suppression factor $S_z^{(a)}/S_z^{(b)} = Q_l^2$ as function of the linearly polarized pulse area Θ_l, taking into account a finite scattering time between different trion states. We introduced it as a negative imaginary part $-i/(2\tau_1)$ of the trion resonance frequency, ω_0, in Eq. (9). The calculated depolarization factor is shown in Fig. 16. It is seen that the Rabi oscillations become less pronounced with increase of τ_p/τ_1 and eventually disappear for $\tau_p/\tau_1 \geq 3$.

The discrepancy of the theoretical predictions and the experimental data for a circularly polarized control results from limitations of the model. We consider the optical transition from a localized electron state to a trion state within a two-level model neglecting completely other excited states such as, e.g., triplet trion states, etc. Their inclusion, see Sec. IV C and thin solid curve in Fig. 14, may result in the complete suppression of the Kerr signal due to the nonadditive contribution of the circularly polarized control pulse. In addition, heating of the electron ensemble can be considerable for

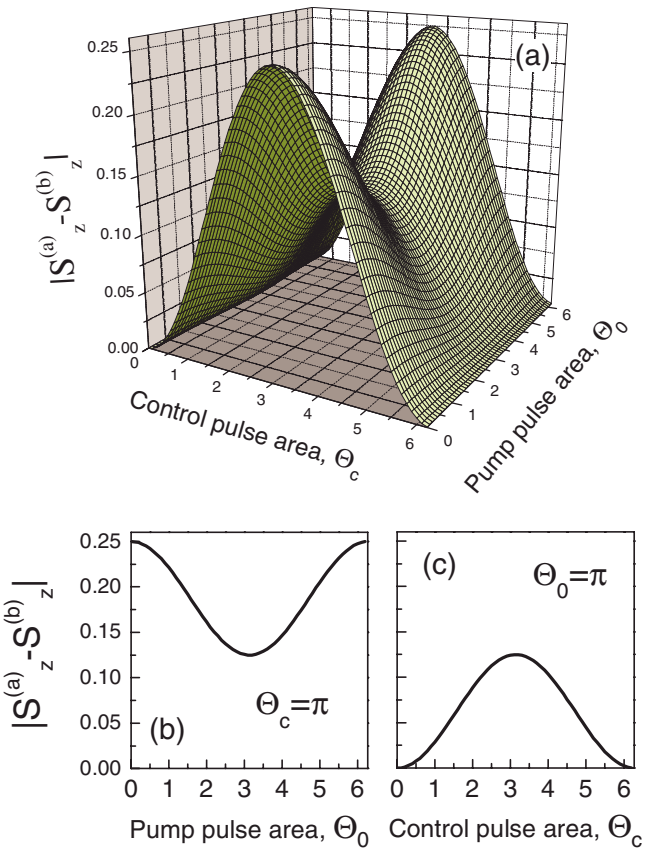

FIG. 17. (Color online) Modification of the spin z component as function of control and pump pulse areas. Panel (a) shows three-dimensional plot. Panels (b) and (c) show its cross-sections for $\Theta_c=\pi$ and $\Theta_0=\pi$, respectively. Calculations performed for co-polarized configuration and $\varphi=0$.

pump powers exceeding 5 $\mathrm{W/cm^2}$ and can cause reduction of the signal both in linear and circular polarization.

C. Efficiency of electron spin manipulation

It is instructive to analyze the efficiency of spin control by circularly polarized pulses. To this end we plot in Fig. 17 the absolute value of the spin z component change caused by the control pulse, $|S_z^{(a)}-S_z^{(b)}|$, as function of control and pump pulse areas using Eq. (16). We assume that the pump and control pulses are co-polarized and that the control pulse arrives at $\varphi=0$ of the spin beats. It is clearly seen that the modification of the spin z component is a nonmonotonous function of the pump and control pulse areas. The control efficiency depends strongly on the pump area. For instance, if the pump area corresponds to a π pulse, $\Theta_0=\pi$, i.e., the pump effect is maximal, the control effect is reduced as compared with the case of $\Theta_0=0$, where the pump is absent. This is a result of the nonadditive effect of the control pulse: if there is already some spin polarization, it is then reduced by the nonadditive effect. In other words, the electron spin projection is limited by $|S_z|\leq 1/2$, therefore, the larger is the spin created by the pump, the weaker is the effect of the control that can be realized.

For the cross-polarized control and pump configuration (or in the case the co-polarized control arrives at $\varphi=\pi$ of the spin beats) the spin z component modification is stronger. Indeed, the nonadditive effect of the control suppresses the spin polarization and the spin coherence added by the control pulse has an inverse sign as compared with the pump-induced one. Therefore, an increase of the control pulse area from 0 to π always increases $|S_z^{(a)}-S_z^{(b)}|$ independent of the pump pulse area, contrary to the co-polarized configuration.

So far, in our theoretical considerations we have neglected the effect of the phase Φ_c in Eqs. (17) and (18) on the electron spin coherence. It follows from these equations that for $\Phi_c\neq 0$ the electron spin can be rotated in the (x,y) plane by the control pulse. Such rotation would gain the finite spin component of the electron spin polarization on the direction of external magnetic field. The rotation depends on the detuning between the control optical frequency and trion resonance frequency. For zero detuning the rotation is absent. The spin rotation angle has different signs for positive and negative detunings.[7,18] Therefore, even for a spectrally broadened control pulse, which is resonant with the trion transition, the effect of rotation vanishes due to the ensemble averaging. Experimental realization of the spin rotation can be also prevented by a short trion scattering time similarly to the suppression of Rabi oscillations, see Sec. V B. It is worth to mention, however, that the spin rotation by the circularly polarized control pulses was realized in undoped GaAs quantum wells at exciton resonance excitation,[21] in CdTe quantum wells at off-resonant trion excitation[8] and in quantum dot ensembles for the trion excitation, where the decoherence is rather weak.[7]

VI. CONCLUSIONS

We have demonstrated experimentally the possibility to manipulate the electron spins in quantum wells by means of polarized laser pulses. We have shown that the coherence of resident electrons can be increased or decreased by a circularly polarized control pulse depending on the pump/control delay and the relative polarizations of the pump and control pulses. This additive effect is a result of spin coherence generation by the control pulse, which may be added to or subtracted from the pump-induced spin coherence.

We have also found a nonadditive effect of the circularly polarized control pulse. This contribution is experimentally detected by a special modulation protocol where the control pulse is not modulated while the pump pulse is modulated and the Kerr signal is detected by a lock-in technique. The measured signal is decreased by the control pulse and the suppression efficiency is determined by the control pulse power only. It is independent of the circular polarization of the control pulse and the amount of spin coherence induced by the pump.

A similar suppression is observed for linearly polarized control pulses which do not generate any spin coherence in our geometry. The suppression efficiency is the same for linearly and circularly polarized pulses at relatively small control powers.

The experimental findings are well explained by the proposed theoretical model which takes into account the forma-

tion of the singlet trion, localized on an imperfection of an *n*-type quantum well, by polarized light. The electron spin left over from the trion after its radiative recombination is depolarized. Since linearly polarized light results in trion formation regardless of the electron spin projection the spin coherence is suppressed. The model describes both the additive and nonadditive effects by circularly polarized control pulses.

The developed model can also be applied to describe the electron spin coherence control in quantum dots. Similarly to quantum well systems studied here, both additive and nonadditive effects of the control pulse should be manifested in that case. One may also expect the observation of Rabi oscillations of spin suppression for the quantum dot systems since the trion state is much more robust and observations of Rabi oscillations have been reported, e.g., in experiments with optical generation of spin coherence in an ensemble of singly charged (In,Ga)As/GaAs quantum dots.[20]

The manifestations of the nonadditive effect are related with the considerable spin polarization generated by the pump pulse, and in general, do not require the trion as an intermediate state in the spin coherence manipulation. The high-spin polarization regime can be achieved for the widely studied quantum wells containing a dense electron gas. However, it occurs at much higher excitation densities where other non-linear effects complicate the interpretation of the experimental data. On the contrary, in quantum wells with a low density electron gas as studied here a relatively high spin polarization can be reached already at rather low-excitation powers.

ACKNOWLEDGMENTS

The authors are grateful to E. L. Ivchenko for valuable discussions. The work was supported by the Deutsche Forschungsgemeinschaft, the EU Seventh Framework Programme (Grant No. 237252, Spin-optronics), the Russian Foundation for Basic Research, the Ministry of Science, and Higher Education (Poland) under Grant No. N202 054 32/1189 and by the Foundation for Polish Science through subsidy 12/2007. One of the authors (M.M.G.) acknowledges support by the President grant for young scientists and the "Dynasty" Foundation—ICFPM.

[1] *Spin Physics in Semiconductors*, edited by M. I. Dyakonov (Springer-Verlag, Berlin, 2008).
[2] *Semiconductor Quantum Bits*, edited by F. Henneberger and O. Benson (World Scientific, Singapore, 2008).
[3] *Semiconductor Spintronics and Quantum Computation*, edited by D. D. Awschalom, D. Loss, and N. Samarth (Springer-Verlag, Berlin, 2002).
[4] D. R. Yakovlev and M. Bayer, in *Spin Physics in Semiconductors*, edited by M. I. Dyakonov (Springer-Verlag, Berlin, 2008), Chap. 6, p. 135.
[5] D. Press, T. D. Ladd, B. Zhang, and Y. Yamamoto, Nature (London) **456**, 218 (2008).
[6] J. Berezovsky, M. H. Mikkelsen, N. G. Stolz, L. A. Coldren, and D. D. Awschalom, Science **320**, 349 (2008).
[7] A. Greilich, S. E. Economou, S. Spatzek, D. R. Yakovlev, D. Reuter, A. Wieck, T. L. Reinecke, and M. Bayer, Nat. Phys. **5**, 262 (2009).
[8] C. Phelps, T. Sweeney, R. T. Cox, and H. Wang, Phys. Rev. Lett. **102**, 237402 (2009).
[9] R. Akimoto, K. Ando, F. Sasaki, S. Kobayashi, and T. Tani, J. Appl. Phys. **84**, 6318 (1998).
[10] E. A. Zhukov, D. R. Yakovlev, M. Bayer, M. M. Glazov, E. L. Ivchenko, G. Karczewski, T. Wojtowicz, and J. Kossut, Phys. Rev. B **76**, 205310 (2007).
[11] G. V. Astakhov, D. R. Yakovlev, V. V. Rudenkov, P. C. M. Christianen, T. Barrick, S. A. Crooker, A. B. Dzyubenko, W. Ossau, J. C. Maan, G. Karczewski, and T. Wojtowicz, Phys. Rev. B **71**, 201312(R) (2005).
[12] T. Wojtowicz, M. Kutrowski, G. Karczewski, and J. Kossut, Appl. Phys. Lett. **73**, 1379 (1998).
[13] E. A. Zhukov, D. R. Yakovlev, M. Bayer, G. Karczewski, T. Wojtowicz, and J. Kossut, Phys. Status Solidi (b) **243**, 878 (2006).
[14] D. R. Yakovlev, E. A. Zhukov, M. Bayer, G. Karczewski, T. Wojtowicz, and J. Kossut, Int. J. Mod. Phys. B **21**, 1336 (2007).
[15] E. A. Zhukov, D. R. Yakovlev, M. Gerbracht, G. V. Mikhailov, G. Karczewski, T. Wojtowicz, J. Kossut, and M. Bayer, Phys. Rev. B **79**, 155318 (2009).
[16] G. V. Astakhov, V. P. Kochereshko, D. R. Yakovlev, W. Ossau, J. Nürnberger, W. Faschinger, G. Landwehr, T. Wojtowicz, G. Karczewski, and J. Kossut, Phys. Rev. B **65**, 115310 (2002).
[17] A. A. Sirenko, T. Ruf, M. Cardona, D. R. Yakovlev, W. Ossau, A. Waag, and G. Landwehr, Phys. Rev. B **56**, 2114 (1997).
[18] I. A. Yugova, M. M. Glazov, E. L. Ivchenko, and Al. L. Efros, Phys. Rev. B **80**, 104436 (2009).
[19] G. V. Astakhov, M. M. Glazov, D. R. Yakovlev, E. A. Zhukov, W. Ossau, L. W. Molenkamp, and M. Bayer, Semicond. Sci. Technol. **23**, 114001 (2008).
[20] A. Greilich, R. Oulton, E. A. Zhukov, I. A. Yugova, D. R. Yakovlev, M. Bayer, and A. Shabaev, Al. L. Efros, I. A. Merkulov, V. Stavarache, D. Reuter, and A. Wieck, Phys. Rev. Lett. **96**, 227401 (2006).
[21] Y. Shen, A. M. Goebel, and H. Wang, Phys. Rev. B **75**, 045341 (2007).